Journal of Environmental Chemical Engineering 13 (2025) 118491

Contents lists available at ScienceDirect

Journal of Environmental Chemical Engineering

journal homepage: www.elsevier.com/locate/jece

Decontamination of high salinity supercritical water gasification wastewater by an integrated electrocoagulation / electrochemical oxidation process

Vasilis C. Sarasidis [a,*], Julian Dutzi [b], Panagiota N. Petsi [a], Konstantinos V. Plakas [a], Nikolaos Boukis [b], Jörg Sauer [b]

[a] Chemical Process and Energy Resources Institute (CPERI), Centre for Research and Technology Hellas (CERTH), 6th km Charilaou-Thermi Road, Thermi, Thessaloniki, GR 57001, Greece
[b] Institute of Catalysis Research and Technology (IKFT), Karlsruhe Institute of Technology (KIT), Eggenstein-Leopoldshafen 76344, Germany

ARTICLE INFO

Keywords:
Supercritical water gasification
Brine treatment
Heavy metals removal
Hybrid method

ABSTRACT

In this work, the treatment of highly saline wastewaters simulating the effluent of the SCWG process was investigated for the first time using a combined process of electrocoagulation (EC) and electrochemical oxidation (EO) in a single set-up. First, EC with different metal electrodes (e.g. Fe, Al, SS) as anode was applied to synthetic wastewater and the effect of operating parameters, such as current density, electrolysis time and pH, on the process performance was systematically studied. Experimental design, statistical analysis and model optimization were carried out to determine the optimum experimental conditions that maximize the removal of lead ions while minimizing energy consumption. According to the results, EC was very effective in the removal of Pb^{2+} as 93 % was achieved under specific conditions (10 mA/cm^2, 9 min, pH 10), while the energy consumption was relatively low at 0.88 kWh/m^3 of treated wastewater. Furthermore, this work provides a performance evaluation of the integrated EC/EO process for the treatment of synthetic or real SCWG brines. EC/EO with two electrode pairs (Fe/Fe and BDD/SS) connected in parallel can achieve complete Pb^{2+} removal at high flow rates (175 ml/min), corresponding to short electrolysis times (9 min), when treating a synthetic SCWG brine, and also performs very well under realistic conditions. In the case of real industrial wastewater, high removal rates of organic and inorganic substances; i.e., approx. 60 % PhOH, 40 % TOC, 75 % Pb^{2+}, 75 % Ni^{2+}, can be achieved after 132 min of electrolysis with 64 mA/cm^2, which demonstrates the very high efficiency of the EC/EO.

1. Introduction

Supercritical water gasification (SCWG) is a hydrothermal conversion process that utilizes water in its supercritical state as a solvent and reactant to convert organic matter into gases [1]. Water in its supercritical state (T > 374 °C, P > 221 bar) is a non-polar solvent in which organic substances dissolve well [2,3]. Additionally, gases dissolve well in the supercritical water [4,5]. The supercritical water thus acts as an optimal reaction medium for homogenous reaction for organics and gases. The organic substances are hydrolyzed according to Eq. (1) [6]. Moreover, gas phase reactions, namely the water-gas-shift reaction (Eq. (2)) and methanation reactions (Eqs. (3) and (4)) take place [7].

$$CxHyOz + (2x\text{-}z)\ H_2O \rightarrow xCO_2 + (2x - z + 0.5y)\ H_2 \quad (1)$$

$$CO + H_2O \leftrightarrow CO_2 + H_2 \quad (2)$$

$$CO + 3H_2 \leftrightarrow CH_4 + H_2O \quad (3)$$

$$CO_2 + 4H_2 \leftrightarrow CH_4 + 2H_2O \quad (4)$$

The main product of the process is a gas composed of mainly H_2, CO_2 and CH_4. CO and C_{2+} compounds are present to a small extent [8]. The excess water leaves the system as wastewater, in case of incomplete gasification together with organics that were not gasified [9].

When processing model biomass compounds, like methanol, ethanol or glycerol, the only two product streams occurring are the product gas and the wastewater [10,11]. However, when processing real biomass like plants, kitchen waste or sewage sludge an additional product stream appears, namely the salt brine [12–16]. The inorganic components in

* Corresponding author.
E-mail address: sarasidis@certh.gr (V.C. Sarasidis).

https://doi.org/10.1016/j.jece.2025.118491
Received 2 May 2025; Received in revised form 18 July 2025; Accepted 3 August 2025
Available online 5 August 2025

the biomass are poorly soluble in supercritical water and thus precipitate in the process [17–19]. In order to avoid deposition in the system that can lead to plugging of tubing the salts need to be separated. Boukis et al. proposed to separate the salts by gravity [20]. The resulting salt brine contains inorganics, like salt building elements and heavy metals, but also some organics from the system.

In order to operate the SCWG process sustainably, the waste streams (wastewater and salt brine) need to be treated in an efficient manner. The wastewater, if it is free of inorganic contaminants, can be recycled to substitute a significant amount of fresh-water needed [8,20,21]. The salt brine contains many different contaminants, organic and inorganic, and thus cannot be directly disposed. Some of the inorganic contaminants like phosphorus or potassium are valuable products themselves [22–23]. To gain these valuable products from the salt brine, first organic contamination and contamination by heavy metals needs to be eliminated. After the treatment of the salt brine (and potentially the regain of nutrients) the water then is disposable.

In the present study, the treatment of such a salt brine originating from the SCWG of plants that were used for phytoremediation in the framework of the H2020 EU-project CERESiS-ContaminatEd land Remediation through Energy crops for Soil improvement to liquid biofuel Strategies [24] is investigated. Possible technologies to remove the heavy metals from the salt brine are electrocoagulation (EC), membrane filtration and adsorption on different materials like zeolites or biochar [25]. On the other hand, the organics in the salt brine could be removed via adsorption, filtration and oxidation, such as electrochemical oxidation (EO) [26,27]. As both, organic and inorganic contaminants need to be treated, a combination of different processes is needed for cleanup of the salt brine.

EC is based upon a process generally referred as “adsorption and co-precipitation”. It consists of generating coagulant species in situ by electrolytic oxidation of sacrificial anode materials triggered by electric current applied through the electrodes. The metal ions generated by electrochemical dissolution of a consumable anode spontaneously undergo hydrolysis in water, depending on the pH, forming various coagulant species including hydroxide precipitates able to remove pollutants by adsorption/settling and other ion metal species (HMs). Besides, simultaneous cathodic reaction allows for pollutant removal either by deposition on cathode electrode or by flotation (evolution of hydrogen at the cathode) [28]. There are numerous studies in the literature that have demonstrated the great effectiveness of the EC process in treating different types of waters and wastewaters, including drinking water [29], river water [30,31], greywaters [32–34], saline waters [35–38] and brines [39]. EC has also been applied successfully to industrial wastewater streams such as those from the textile [40–42], tannery [43,44], metal-plating [45], olive mill [46] and pulp and paper [47] industries, among others [48–50]. A substantial number of publications focus on the use of EC for the efficient removal of various pollutants, including dyes [51,52], heavy metals [53–56], organic compounds [57–59] and specific ions [31,60]. Additionally, several interesting and critical reviews [28, 61–68] on the mechanisms, electrode materials and arrangement, key operational parameters, and energy considerations of EC have been provided.

In EO, hydroxyl radicals (•OH) can be generated by direct electrochemistry (anodic oxidation, AO) or indirectly through electrochemically generation of strong oxidants in the brine. In the first case hydroxyl radicals are generated heterogeneously by direct water discharge on the metal anode (M) (Eq. (5)), while in the last case strong oxidants are generated in situ indirectly in the bulk (persulfate and active chlorine species by Eqs. (6) and (7)) thus favoring the oxidation of the organic compounds in shorter time [69].

$$M + H_2O \rightarrow M(\bullet OH) + H^+ + e^- \quad (5)$$

$$2SO_4^{2-} \rightarrow S_2O_8^{2-} + 2e^- \quad (6)$$

$$2Cl^- \rightarrow Cl_2(g) + 2e^- \quad (7)$$

EO requires high oxidation power anodes; i.e., anodes with high O_2 overpotential to minimize the extent of O_2 evolution from Eq. (8) [70].

$$2\,M(\bullet OH) \rightarrow 2\,M + O_2 + 2H^+ + 2e^- \quad (8)$$

Anode materials such as graphite, platinum, metal oxides, and Boron-Doped Diamond (BDD) are usually preferred. Among the different electrode materials tested in literature, the oxidative action of M(•OH) is much more efficient in the case of BDD anodes [71]. It has been found that operating at a high current, within the water discharge region, reactive BDD(•OH) is produced in much higher quantities than Pt(•OH) and can completely mineralize aromatics and unsaturated compounds such as carboxylic acids [72]. Furthermore, the low adsorption ability of •OH on BDD favors its dimerization to H_2O_2 by Eq. (9), whereas the high oxidation power of this anode facilitates the generation of ozone from water discharge by Eq. (10) and other weaker oxidizing agents such as $S_2O_8^{2-}$ ion from oxidation of SO_4^{2-} ions from Eq. (6) when sulphate medium is employed [73].

$$2BDD(\bullet OH) \rightarrow BDD + H_2O_2 \quad (9)$$

$$3H_2O \rightarrow O_3(g) + 6H^+ + 6e^- \quad (10)$$

The combination of the two well-known electrochemical techniques stem from the high electrical conductivity (eC) and the presence of inorganic ions (e.g. sulphates, chlorides) in the saline SCWG wastewater which result to reduced energy consumption (due to the decreased ohmic resistance of the brine and thus, the low voltage that needs to be applied), and to the in situ production of chemical reagents (e.g. coagulants, strong oxidants) for the scope of the separation/elimination of the target contaminants. The parameters affecting the effectiveness of the two processes have been systematically investigated. These are related to a) the operating conditions such as current density and treatment time, b) the brine wastewater chemistry such as pH, alkalinity and eC and c) the geometry of the EC/EO reactor and the EC/EO electrodes (electrode surface, electrode spacing). The integration of EC with EO has gained increasing interest for advanced treatment. Researchers like Linares-Hernández et al. [49,74], Gengec [75], Azarian et al. [76] and Benekos et al. [77] have investigated hybrid EC/EO systems to enhance the degradation of industrial wastewaters and the treatment of nitrate-polluted groundwater respectively. These studies confirm that EC in combination with EO, is a promising technology for treating complex wastewaters containing emerging and/or hazardous contaminants. Although these studies confirm that EC in combination with EO, is a promising technology for treating complex wastewaters containing emerging and/or hazardous contaminants, the processes were implemented sequentially, since EC is applied first, followed by EO as a post-treatment step rather than simultaneously. Furthermore, none of the aforementioned studies achieved inorganic and organic decontamination of the feed solution at the same time; instead, they reported only the individual removal of Chemical Oxygen Demand (COD) and Total Organic Carbon (TOC) [49, 74–76], or NH_4^+ [77]. While extensive research has been also conducted on the various applications of electrocoagulation, to the best of the authors’ knowledge no previous studies have addressed the use of EC process for the decontamination of SCWG effluents, particularly in conjunction with EO within a single unit at a pilot-scale. In the present study, a hybrid process integrating EC and EO in the same experimental set-up is investigated for the combined removal of inorganic and organic contaminants. Such a hybridization offers a compact system (since EC and EO share the same electrolysis vessel) that consumes lesser energy with similar to the literature removal kinetics. The integrated approach used here enables potential advantages such as a reduced system footprint and the concurrent occurrence of all phenomena (e.g. coagulation, precipitation, flotation, oxidation, etc.). Lead and phenol were chosen as inorganic and organic model pollutants respectively, in simulated and real SCWG wastewater to assess the suitability of the technology.

2. Experimental

2.1. Preliminary SCWG experiments

Preliminary SCWG experiments were carried out to produce the salt brine needed for the performance evaluation of the EC/EO process. A detailed description of these experiments can be found in previous work [13].

2.1.1. Experimental set-up

The SCWG experiments are conducted in the LENA lab-plant. LENA is a German acronym for "Laboratory plant for energetic utilization of agricultural materials". The LENA plant is a high pressure ($P \leq 300$ bar) - high temperature ($T \leq 700°C$) plant constructed for continuous SCWG experiments. It consists of three sections: (i) the feed system, (ii) the reaction system and (iii) the product collection section. A short description follows, for further details see [13].

i. The biomass slurry is stored in a pressurized cylinder from which it is indirectly pumped into the reaction system by a water-driven piston (for details see [8]). The pumps are regulated by a mass flow controller that is set to the desired mass flow of biomass slurry.
ii. The reaction system consists of the preheater and the gasification reactor followed by a filter for collection of salt brine. In the preheater the biomass slurry is heated to about 350°C before it enters the gasification reactor. The preheater is made of a SS316 pipe (750 mm length, 8 mm inner diameter, 9/16-inch outer diameter) that is heated electrically from the outside of the pipe. The gasification reactor is downstream of the preheater. It is made of the nickel-base alloy 625 (1500 mm length, 8 mm inner diameter, 9/16-inch outer diameter) and also heated from the outside by electric heaters. In the reactor temperatures of 650°C are reached to gasify the organics in the biomass. Solids and tars that formed in the gasification process can be collected in the filter bearing downstream of the reactor. Additionally, some inorganics that are poorly soluble in supercritical water and thus precipitated in the reactor might redissolve and can be retracted from the filter bearing as salt brine. The separation is realized via a sluice installed at the bottom of the filter bearing. At this point, two needle valves, opening 20 ms apart from each other, act as a sluice and retract about 3 ml of salt brine every 5 min.
iii. Three product streams leave the system. The salt brine is retracted from the filter bearing as described in section (ii) and collected in a glass container that is placed on a scale (Soehnle Industrial Solutions GmbH) to monitor the retracted mass. The product gas and the reactor effluent pass the back-pressure regulator, provided by Tescom. The gas is quantified using a gas meter (Ritter Apparatebau GmbH % Co. KG), while the effluent is also collected in a separate glass container and weighed (Soehnle Industrial Solutions GmbH). Gas and liquid samples can be taken throughout the experiment to evaluate the steady-state operation of the experiment.

2.1.2. Preparation of educts

The SCWG experiments evaluated in this paper were conducted with eight different biomasses: Panicum virgatum (PV), Arundo donax (AD), Miscanthus (MC) – grown at two sites (abbreviated by ST and HH), Short rotation coppice (SRC) – grown at two sites (abbreviated by ST and HH), Sugar cane (SCane) and Energy cane (ECane). These biomasses were provided by CERESiS partners from Scotland, Italy and Brazil. The biomasses were used for phytoremediation on contaminated sites and show low levels of contamination themselves. The maximum concentration of the analyzed heavy metals in the feed slurry, based on dry matter, is displayed in Table 1.

Part of the biomasses were delivered in form of a powder ($\leq$0.25 mm grain size). The rest of the biomasses were milled to a size of 0.2 mm or smaller by a mill (Pulverisette 14, Fritsch GmbH). The two slightly different grain sizes did not affect the process.

The biomass powder was mixed with distilled water to create a feed slurry with a dry matter content of 8 wt %. Xanthan (Carl Roth GmbH) was added as a thickening agent (0.5 wt %) and KOH (Merck KGaA) was added as a homogeneous catalyst, in varying concentration (see Fig. 1). The feed was thermally pretreated in a mixer at $T = 70°C$ (Thermomix Tm31, Vorwerk Deutschland Stiftung & Co. KG). The dry matter content was determined by drying the sample at 105°C in an oven for 24 h.

In some experiments, methanol (MeOH) (Merck KGaA) was added to the feed slurry before the experiment as a molecule that is easily gasified under SCWG conditions. By the decomposition of MeOH hydrogen is formed. Thus, hydrogen is present early in the process. With this addition the influence of a hydrogen donor on the process was assessed.

The concentrations of the added K^+ and MeOH are given in Table 2. 13 experiments are evaluated in this work regarding the gasification process in a prior publication by Dutzi et al. [13], except for Exp. No 13 which had a similar gasification outcome like the other experiments. In Table 2, for orientation purposes, the reference to the experiment numbers in the previous publication [13] is also provided, with the exception that the salt brines of Exp. No 8 and 13 in [13] were not used and, therefore are not listed here.

2.1.3. Experimental procedure

The lab-plant was pressurized using water and subsequently heated to the desired temperatures. A day before the experiment with the CERESiS biomasses, a preliminary experiment with 5 wt % ethanol (EtOH) solution (C_2H_6O, VWR Chemicals) was conducted. By this procedure the system could be checked for leaks and additionally a gas-liquid equilibrium in the lab-plant was reached. Dead volumes were filled with water-gas mixtures similar to those present in the actual experiment. Thus, steady state could be reached faster when the CERESiS biomasses were processed.

The feed slurry was stored inside a pressurized tank prior to the start of the experiment. By coupling the tank to the system, the feed slurry was pumped indirectly by a water driven piston into the lab-plant. The experiment was conducted for up to eight hours, if pressure drop did not increase or no leakages occurred. In time intervals of 30 min gas samples were collected and analyzed. Liquid samples were also collected throughout the experiments. Steady state operation was determined by constant gas flow and gas composition. After the experiment, the system

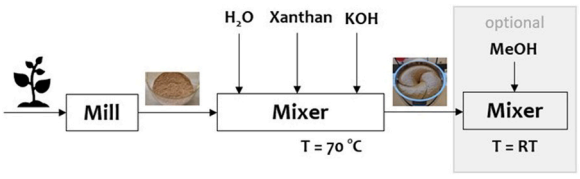

Fig. 1. Feed slurry production scheme.

Table 1
Maximum heavy metal contamination of feed slurries based on dry matter.

Cd (wt%)	Co (wt%)	Cr (wt%)	Cu (wt%)	Fe (wt%)	Hg (wt%)	Mn (wt%)	Ni (wt%)	Pb (wt%)	Zn (wt%)
ND[a]	ND	0.003	0.01	0.039	ND	0.084	0.002	ND	0.017

[a] Not Detected

Table 2
Feed production parameters of conducted experiments.

Exp. No.	Exp. No [13]	Biomass	K^+ (mg/kg Feed)	MeOH (wt%)
1	1	PV	0	2
2	2	PV	1000	2
3	3	PV	3000	2
4	4	PV	5000	2
5	5	PV	5000	-
6	6	SCane	5000	-
7	7	AD	5000	-
8	9	ST-MC	5000	-
9	10	ST-SRC	5000	-
10	11	HH-MC	5000	-
11	12	HH-SRC	5000	-
12	14	ECane	5000	-
13	-	PV	5000	1

was flushed by water to clean it. Additionally, if the pressure drop increased during the experiment, the lab-plant was checked for solid deposits that were mechanically removed if present.

In all experiments the reaction temperature was 650°C and the pressure was 280 bar. The flow rate was set to 200 g/h. In intervals of 300 s the salt brine was retracted via a sluice.

2.1.4. Analysis

The gas samples obtained from the product gas are subjected to immediate analysis using the gas chromatograph 5890 series II plus (Hewlett-Packard GmbH), equipped with a fused silica capillary column (Carboxen 1010 PLOT 30 m, SUPELCO). The thermal conductivity and flame ionization detectors are utilized to determine the volume fractions of gas components, namely H_2, CO, CH_4, CO_2, C_2H_4, C_2H_6, C_3H_8 and C_3H_6. The Total Carbon (TC) content in liquid samples is determined through combustion, while Total Inorganic Carbon (TIC) is extracted through acid extraction in a Total Organic Carbon (TOC) analyzer (DIMATOC 2100, DIMATEC Analysentechnik GmbH). TOC is then calculated by subtracting TIC from TC. The content of organic species in the liquids is analyzed via HPLC analysis with different columns (Lichrosper 100 RP-18, by Merck; Kinetex 2.6 µl C18 PFP 100 A 100 × 4.6 (OOD-4462-EO), by Phenomenex; Aminex HPX 87H, by Biorad). The concentration of trace elements, such as Al, Ca, Cr, Cu, Fe, K, Mg, Mo, Na, Ni, S, Si, and Zn, is determined using ICP-OES (Inductively Coupled Plasma-Optical Emission Spectrometry) with an Agilent 725 spectrometer (Agilent Technologies).

2.2. EC and EC/EO experiments

The experiments in this study were conducted either with the EC alone or with the combined EC/EO oxidation process. The EC experiments were carried out prior to those involving the combined EC/EO process.

2.2.1. Materials and reagent

In this study, a total of four metal plates were used as cathode and anode electrodes for EC and EC/EO experiments. Iron (Fe), aluminum (Al) and Stainless Steel (SS) plates were tested in the case of the EC process, while Boron Doped Diamond (BDD) plate was used as anode electrode only in the case of the EC/EO process. The dimensions of the Fe, Al and SS plates (VETA S.A, Greece) were 10 × 10 × 3 cm, corresponding to an effective surface area of 100 cm^2 each, while the BDD plate (ElectroCell A/S, Denmark) was smaller at 7 × 4.5 × 3 cm and had a surface area of 31.5 cm^2. Phenol (C_6H_5OH, Sigma Aldrich) and lead (II) in the form of lead nitrate ($Pb(NO_3)_2$, Sigma Aldrich) were used as target pollutants to simulate the organic and inorganic contamination of a SCWG effluent, respectively. In addition, potassium chloride (KCl, Merck) and potassium carbonate (K_2CO_3, Baker) were used as electrolytes to achieve the desired electrical conductivity of the synthetic simulated solution, while a 1 M buffer solution of hydrochloric acid (HCl, Fluka) was used for pH adjustment. The water matrix for the preparation of the feed solutions was deionized water (5.2 pH, < 5 µS/cm eC, < 0.1 mg/L TOC). In the case of the experiments with real wastewater, a concentrated salt solution provided by KIT was used. This specific brine was a mixed solution from a series of 13 experiments performed at KIT and the results of the analysis of the mixture measured at KIT and CERTH prior and after transportation respectively are shown in Table 3.

2.2.2. Experimental set-up

The same experimental setup was used for both processes. Fig. 2 shows a schematic diagram and an image of the special laboratory pilot unit, designed and built at CPERI/CERTH's Natural Resources and Renewable Energies (NRRE) laboratory. It mainly consisted of three vessels made of Plexiglas®, namely the cylindrical 5-liter feed vessel, the rectangular 1.6-liter electrolysis vessel with a V-shaped bottom, and the rectangular 3.4-liter sedimentation vessel with a V-shaped bottom. Two metal plates of Fe, Al or SS forming a pair of electrodes; i.e., Fe/Fe, Al/Fe or SS/Fe, were used each time EC experiments were performed. In contrast, in the integrated EC/EO method, four metal plates of Fe, SS and BDD, forming two pairs of electrodes; i.e., Fe/Fe and BDD/SS, were placed in the electrolysis vessel and were connected in parallel. The distance between the electrodes was fixed at 2 cm, based on values found in prior publications [32,37,46,51]. The EC/EO unit was also equipped with a piston pump operating at a volumetric rate of 25–200 ml/min for recirculation of the feed solution, a flow meter, various sensors and transmitters for monitoring pH, temperature and electrical conductivity, a magnetic stirrer for homogeneity of the feed solution and a DC power supply of 0–30 V / 0–5 A for current application. Finally, a data acquisition system consisting of a Programmable Logic Controller (PLC) with a touch screen and a Human-Machine Interface (HMI) was used to record the data and for general control of the unit.

2.2.3. Experimental procedures

First, a synthetic feed solution was prepared to simulate an SCWG effluent. For this purpose, a concentrated phenol (PhOH) stock solution was prepared and a certain volume of the stock solution was diluted with deionized water to a final volume of 5 L to achieve the desired concentration of organic matter; i.e., 200 mg/L as PhOH. In addition, appropriate amounts of KCl and K_2CO_3 salts were added to the above diluted solution in a mass ratio of 10/90 % w/w, corresponding to a concentration of 4 mM and 19.6 mM, respectively, to obtain the desired value of eC; i.e., about 4.5 mS/cm. Finally, lead ions were added to this mixture to simulate the heavy metal load of the SCWG wastewater; i.e., 6–7 mg/L as Pb^{2+}. The simulated solution was then added to the feed vessel and magnetically stirred at 800 rpm for 10 min to ensure homogeneity. At that point a pH adjustment took place if needed, by adding the appropriate volume of the buffer solution. In the case of the

Table 3
Physicochemical characterization of the real brine.

pH[a]	eC[a] (mS/cm)	COD[a] (mg/L)	TOC[a] (mg/L)	TSS[a] (mg/L)	Pb^{2+}[b] (mg/L)	Ni^{2+}[b] (mg/L)
8.62	3.32	2775	822	79	ND[b]	1.98

Al^+ (mg/L)	Na^+ (mg/L)	K^+ (mg/L)	Ca^{2+}[b] (mg/L)	Mg^{2+}[b] (mg/L)	Si^{2+}[b] (mg/L)	P (mg/L)
0.70	11.7	868	12.9	1.19	33.5	6.30

S (mg/L)	PhOH[a] (mg/L)	EtOH (mg/L)	Resorcinol (mg/L)	Formic Acid (mg/L)	Acetic Acid (mg/L)	Glucose (mg/L)
6.90	411	50.0	30.4	134	67.0	82.0

[a] measured at CERTH after transportation
[b] Not Detected

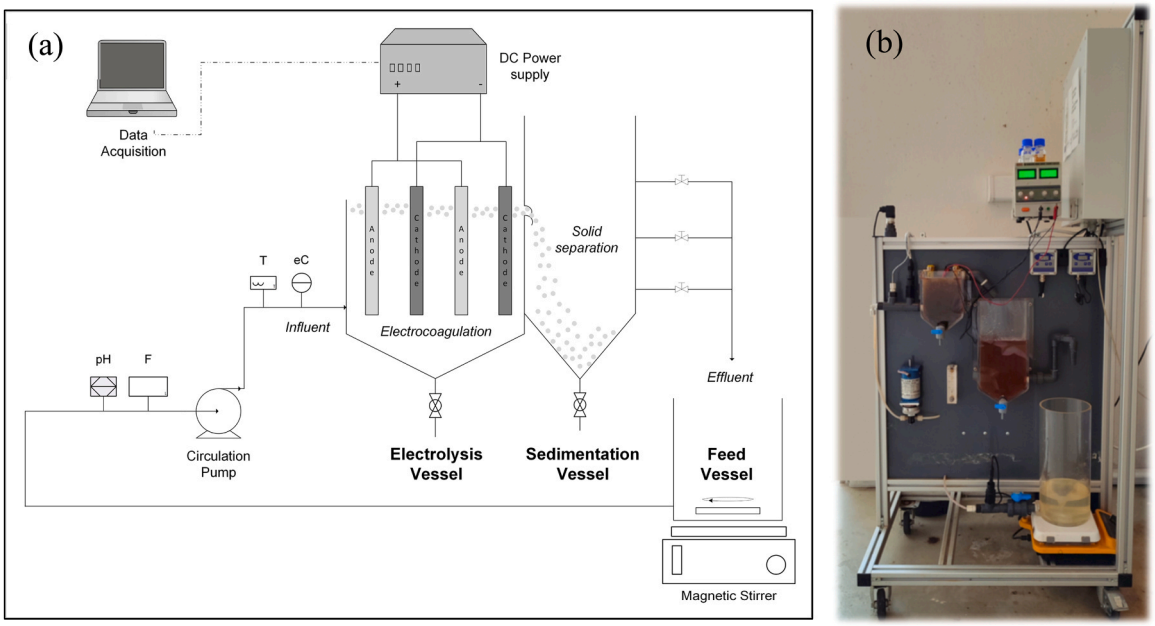

Fig. 2. (a) Schematic diagram and (b) front view of the EC/EO laboratory-pilot unit.

experiment with real SCWG wastewater the pilot unit was fed directly with 2.75 L of the brine sample. The simulated or real feed solution was then fed into the electrolysis vessel using the circulation pump, into which the one or two pairs of electrodes, arranged in parallel, to each other were immersed. As soon as the electrodes were completely covered by the feed solution, the power supply was switched on, an electric current was applied and the experiment began (treatment time t = 0). Since the electrodes were connected in parallel (as in the EC/EO method), the applied current was divided equally between the two pairs of electrodes; i.e., between the two anodes (Fe and BDD), resulting in a smaller potential difference than if the electrodes were connected in series. During the experiment, coagulation, flotation and precipitation phenomena took place in the electrolysis and sedimentation vessels, as well as the production of gases (e.g. CO_2, O_2 and H_2) by electrolysis, while the supernatant from the electrolysis vessel was carried by flotation into the sedimentation vessel where it settled. In addition, the supernatant flowed over from the sedimentation vessel and returned to the feed vessel. At certain intervals, samples were taken from feed and sedimentation vessels for analysis. At the end of each experiment and before the next one, the equipment (vessels, pipes, etc.) was thoroughly rinsed with fresh, clean water. The BDD anode electrode was cleaned using acetone to remove residues, while the Fe, Al, SS anode and Fe cathode electrodes were replaced with new ones.

2.2.4. Analytical methods and measurements

A UV-Vis spectrophotometer (Spectroquant® Pharo 100, Merck) was used either for colorimetric measurement of PhOH concentration according to ISO standard 6439 or for scanning the total spectra of the samples. A TOC analyzer (TOC-L CSH/CSN, Shimadzu Europa GmbH) was used for the concentration measurements of TOC of the samples and an inductively coupled plasma optical emission spectrometer (ICP-OES, Perkin Elmer) for the concentration determination of lead (Pb^{2+}) and nickel (Ni^{2+}) ions. In addition, turbidity of samples was measured directly (without pretreatment) using a portable turbidimeter (DRT-15CE, HF Scientific™), while measurement of total suspended solids (TSS) of selected samples was performed using an furnace (MMM Medcenter™, Venticel 55) and a balance (AT 201, Mettler Toledo), including filtration with 1.5 μm glass fiber filters and drying at 105°C for 1 h, according to APHA Standard Methods 2540D.

2.2.5. Design of experiments using response surface methodology

At the beginning an experimental design and optimization of the EC process was performed, also known as Design of Experiments (DOE), with the aid of the Design-Expert® Version 11 software. DOE is a systematic and statistical approach for investigating experimental responses while optimizing the number of experiments required. The aim is to collect a maximum amount of information with a minimum number of experiments while ensuring accuracy and efficiency. The selection of the appropriate model based on the objective, the number of factors and the measurement accuracy is crucial. After planning, the experiments are carried out and the collected data is statistically analyzed. The choice of design depends on the proposed model, study objectives, and research focus [78]. In this particular study, a Quadratic Central Composite Design with three factors; i.e., current density (CD) (Factor 1), electrolysis time (ET) (Factor 2), and pH (Factor 3), and two responses; i.e., maximum Pb^{2+} removal (Response 1) and minimum energy consumption (Response 2), were used at one level. Each of the three independent variables was varied at three levels across 16 experimental runs, as detailed in Table 5 of subsection 3.2.1.

The electrolysis time is calculated on the basis of the volume of the electrolysis vessel and the feed rate of the treated solution. The two evaluated responses to assess the performance of the EC process, the percentage removal of Pb^{2+} (Pb^{2+} removal) and the energy consumption (EnC), were calculated from Eqs. (11) and (12), respectively:

$$Pb^{2+}removal\ (\%) = \frac{Pb_o - Pb_t}{C_o} \times 100 \tag{11}$$

where Pb_o (mg/L) is the initial concentration of lead ions in the feed solution and Pb_t (mg/L) is the concentration of lead ions in samples at electrolysis time t.

$$EnC\left(\frac{kWh}{m^3}\right) = \frac{E_{cell} \times I \times t}{V_s} \tag{12}$$

where E_{cell} (V) is the median voltage being recorded during the experiment, I (A) is the applied current, t (h) is the treatment time and V_s (L) is the treated volume of the feed solution.

Response Surface Methodology (RSM), a widely used statistical technique for optimization, was used to optimize the operating parameters. RSM explores the relationships between multiple operational

variables and one or more response variables [78]. The optimization of operating parameters aimed to maximize Pb^{2+} removal and minimize EnC while ensuring that all parameters remained within their original range.

3. Results and discussion

3.1. Production of salt brine via SCWG

The gasification was evaluated in a previous publication by Dutzi et al. [13]. A short summary follows: In general, the kind of biomass processed did not affect the outcome of the experiments, most likely due to their similar elemental composition. Methanol addition did not lead to an increase in gasification efficiency of the biomass. Increased potassium addition in form of KOH increased the gasification efficiency, however it was still far from complete gasification (75 % of carbon was gasified in the best case). The salt separation did not sufficiently separate the salts, deposits in the reaction system occurred. Relevant for the present work is the salt brine generated from these experiments. As expected, the salt brine contains salt building elements. The concentrations of the most salt building elements are below 100 mg/L (see Fig. 3). The only exception is K^+, which is added to the feed slurry as homogenous catalyst. Regaining the potassium in the salt brine would be of great interest for the economics of the process and thus freeing the salt brine from the organic and heavy metal contamination is necessary.

Some small amounts of heavy metals can be found in the salt brines (Table 4). The highest concentrations are present in nickel. This is most likely due to corrosion of the reactor that is made of the nickel-base alloy 625. During the experiments corrosion was visible. Moreover, some of the chromium and iron might originate from the reactor material. Other than these metals, which may potentially originate from the reactor alloy, low concentrations of zinc (< 0.1 mg/L) and manganese (< 0.2 mg/L) are also present. Thus, the subsequent electrocoagulation process needs to mainly focus on the nickel in the present case.

Apart from the inorganic contaminants also some organic compounds are also present in the salt brine. On average, 1256 mg/L total carbon (TC) can be found in the salt brine, consisting of 918 mg/L total organic carbon (TOC) and 338 mg/L total inorganic carbon (TIC). The organic carbon consists of several species, as can be seen in Fig. 4. Sucrose and glucose are formed when cellulose is decomposed. Further decomposition products of cellulose are alcohols (EtOH, MeOH) and carboxylic acids (formic and acetic acid) [7,79]. Decomposition products of lignin are also present, namely resorcinol and phenol [7]. These lignin decomposition products are toxic and hazardous [80,81] and need to be removed in order to safely dispose of the water. Accordingly, here should lie the focus of the later treatment by electrochemical oxidation.

Over the course of the 13 experiments, salt brines were collected separately and then mixed into one container for its treatment by the integrated EC/EO process. The analysis of this salt brine mixture can be found in Table 3.

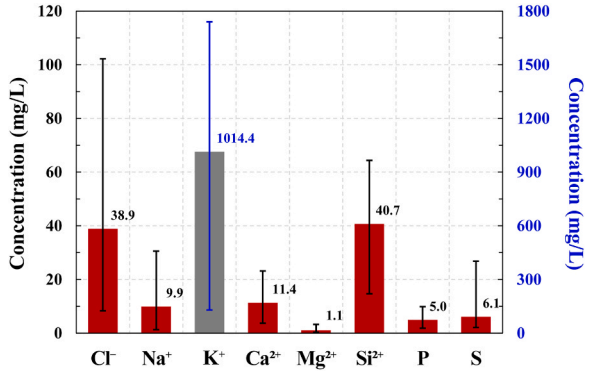

Fig. 3. Average concentration of salt building elements of the different salt brine samples.

Table 4
Heavy metal analysis of the salt brines.

Exp. No	Cr (mg/L)	Ni (mg/L)	Zn (mg/L)	Mn (mg/L)	Fe (mg/L)
1	ND[a]	1.19	< 0.1[b]	< 0.1[b]	< 1.0[b]
2	ND	1.80	< 0.1[b]	< 0.1[b]	< 1.0[b]
3	ND	4.72	< 0.1[b]	0.1	ND
4	ND	5.77	< 0.1[b]	< 0.1[b]	ND
5	ND	5.54	< 0.1[b]	< 0.1[b]	ND
6	ND	ND	ND	< 0.2	ND
7	ND	9.17	< 0.1[b]	< 0.1[b]	ND
8	< 0.4[b]	1.49	< 0.1[b]	< 0.1[b]	ND
9	< 0.4[b]	2.59	< 0.1[b]	< 0.1[b]	ND
10	ND	1.18	< 0.1[b]	< 0.1[b]	< 1.0[b]
11	< 0.4[b]	1.92	< 0.1[b]	< 0.1[b]	ND
12	ND	< 2.0	ND	< 0.2	ND
13	ND	7.09	< 0.1[b]	0.1	ND

[a] Not Detected,
[b] value below quantification limit

This brine serves as a basis for testing the EC/EO setup under application relevant conditions. This salt brine is representative of the SCWG process of plants like the ones processed for this publication and thus the following salt brine treatment can be tested for such conditions. However, when other feedstocks are processed, like sewage sludge that is of special interest for the industry [82], higher concentrations of heavy metals will probably be present in the salt brine due to the higher content in the feed material [83].

3.2. Electrocoagulation

To determine the optimal experimental conditions for the efficient treatment of simulated high saline wastewater from the SCWG process by electrocoagulation, an experimental design, statistical analysis, and process optimization were conducted as follows.

3.2.1. Experimental design

The three independent variables varied at three levels within the specified ranges as shown for each of the total 16 experiments performed along with the corresponding results in Table 5. Thus, the CD held the values 10, 30 and 50 mA/cm^2, the ET 9, 37.5 and 66 min and the pH 5, 7.5 and 10, respectively. These values were determined by preliminary tests (data not shown) conducted in accordance with the capabilities of the implemented equipment and are in agreement with typical values documented in previous studies.

3.2.2. Statistical analysis of results

The experimental data were statistically analyzed and fitted to the optimum mathematical models. Employing the Design-Expert® software, the following Reduced Quadratic Models; i.e., Eqs. (13) and (14) best correlated the two responses (Pb^{2+} removal and EnC) with the three independent variables.

$$Pb^{2+}removal = 90.681 - 0.63 \times ET + 1.19 \times pH + 0.0092 \times ET^2 \quad (13)$$

$$EnC = 22.64 + 22.30 \times CD + 18.59 \times ET + 1.86 \times pH + 15.91 \times CD \times ET + 1.23 \times CD \times pH + 3.48 \times CD^2 \quad (14)$$

The Pb^{2+} removal and EnC models were validated by analysis of variance (ANOVA) and the results are summarized in Table S1 and S2 in the Supplement. The model for Pb^{2+} removal was statistically significant overall (F-value=6.20, p-value=0.0087), with pH and the quadratic term of ET having a notable impact (p-value=0.0453 and 0.0049

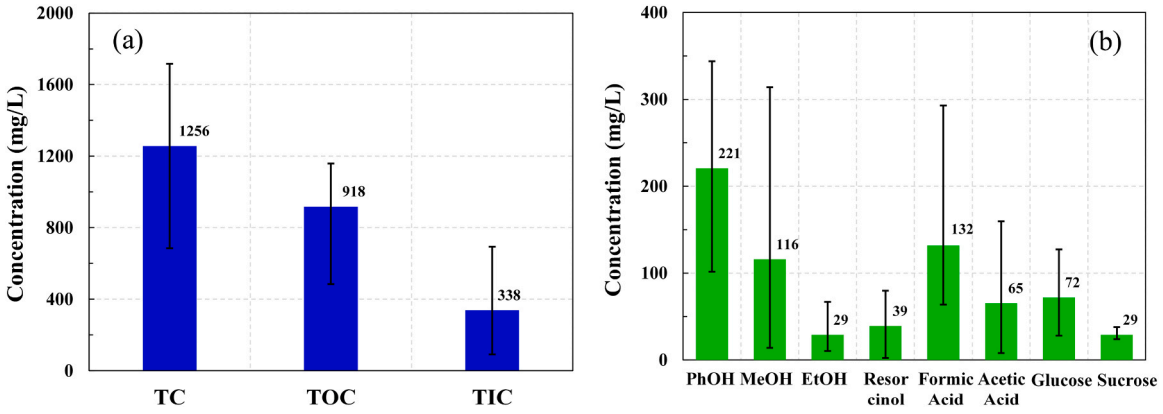

Fig. 4. Average concentration of (a) carbon and (b) organic species in different salt brines.

Table 5
Design of experiments and results of the EC process.

	Factor 1	Factor 2	Factor 3	Response 1	Response 2
Exp. No	**Current Density (mA/cm^2)**	**Electrolysis Time (min)**	**Initial pH**	**Pb^{2+} removal (%)**	**Energy Consumption (kWh/m^3)**
1	10	9	10	97.5	0.88
2	50	66	5	92.4	79.6
3	10	66	10	100	8.11
4	50	66	10	98.8	87.7
5	50	37.5	7.5	92.6	47.4
6	30	9	7.5	98.4	5.22
7	30	37.5	10	94.7	24.7
8	30	37.5	7.5	88.2	23.7
9	10	9	5	84.5	0.85
10	50	9	5	94.0	11.9
11	50	9	10	99.1	15.5
12	10	37.5	7.5	80.8	3.15
13	30	66	7.5	100	38.6
14	30	37.5	5	89.4	19.7
15	30	37.5	7.5	88.2	23.7
16	10	66	5	100	6.20

respectively). The model showed a moderate fit (R^2=0.61) and acceptable adequate precision (7.22) within the experimental data. Despite a relatively low predicted R^2 (0.31), which suggests that additional data may be needed to improve its predictive accuracy, the model remains valid and reliable for trend interpretation. The model for EnC (F-value=748.72, p-value<0.0001) showed excellent fit and predictive power, with a very high R^2= 0.998 and strong agreement between adjusted R^2 (0.997) and predicted R^2 (0.991). All key factors and their interactions were statistically significant (p-values<0.05), while the high adequate precision (84.37) confirms a strong signal-to-noise ratio. The model is highly reliable for both interpretation and prediction. Moreover, the statistical significance of the models is confirmed by Fig. S1 and S2 in the Supplement. In particular, the actual values of Pb^{2+} removal are randomly distributed around the mean of the predicted values, while in the case of EnC there is no scatter between the experimental calculations and the predicted values, indicating complete agreement.

3.2.3. *Optimization of operational parameters*

Based on the results from the experiments listed in Table 5, response surfaces were created using Design-Expert® software. These surfaces, represented by three-dimensional (3D) plots, illustrate the relationship between two operational parameters while the third parameter is held constant.

Figs. 5a and 5b show the 3D plots of the Pb^{2+} percentage removal and energy consumption as a function of the current density and electrolysis time, with the pH value kept constant at 10. From these graphs, predictions can be made about the Pb^{2+} removal and the EnC for certain combinations of current density and electrolysis time. As for the color

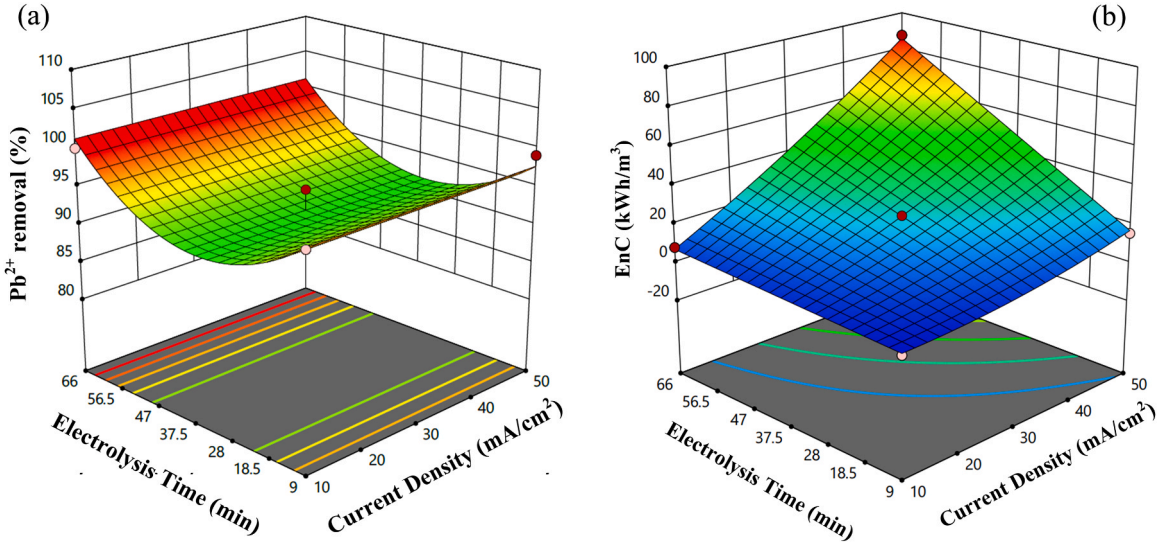

Fig. 5. (a) Pb^{2+} percentage removal and (b) EnC as a function of electrolysis time and current density (at pH 10) during treatment with EC process.

spectrum on the graphs, the maximum values of the two responses (Pb^{2+} removal 100 % and EnC 87.7 kWh/m^3) are shown in red, the minimum values (Pb^{2+} removal 80.8 % and EnC 0.85 kWh/m^3) in blue, and the intermediate values for the percentage removal of Pb^{2+} and energy consumption in the colors in between. From Fig. 5a it can be observed that the optimum range for Pb^{2+} removal corresponds to very short or very long electrolysis times (9 min or 66 min), regardless of the current density values, while Fig. 5b shows that the optimum range for energy consumption corresponds to very short electrolysis times (9 min) and lower current density values (10 mA/cm^2), as expected.

Using Design-Expert® software, a total of 71 highly selective solutions with desirability over 0.83 % were generated as part of the optimization process (Table S3). Among these solutions, solution No 33 was selected as it had a remarkably high Pb^{2+} removal (97.68 %), which was only 2.3 % less than the maximum achievable value, while also having the lowest EnC (1.79 kWh/m^3) compared to the other solutions, 74 % less than solution No 1. The desirability of the optimal solution was 0.954, and the corresponding values of the operating parameters were current density 10 mA/cm^2, electrolysis time 9 min and pH 10.

3.2.4. Effect of anode material on EC performance

To further investigate the performance of the EC process, different anode materials were tested. The sacrificial electrode pairs Al/Fe and SS/Fe were used as a comparison alongside the Fe/Fe pair. The EC experiments (Exp. No 17–19) were performed under the previously established optimum operating conditions and the results are presented in Table 6.

From the results in Table 6, it can be seen that the Fe/Fe electrode pair outperforms the Al/Fe and SS/Fe pairs. In particular, the Fe/Fe pair exhibits a significantly higher percentage of lead removal compared to Al/Fe, while both are superior to the SS/Fe pair. This significant difference in Pb^{2+} percentage removal efficiency between Fe and Al anode electrodes can be probably explained by the higher adsorption capacity of the iron hydroxides, formed during the EC process, compared to aluminum hydroxides. Particularly, these iron hydroxides, (e.g. $Fe(OH)_3$) acting as coagulants, are more effective than $Al(OH)_3$ under these specific conditions due to their greater Pb^{2+} adsorption capacity, which promotes enhanced aggregation and the formation of larger, easily precipitable flocs, thereby increasing Pb^{2+} removal efficiency. In other words, the low solubility of $Fe(OH)_3$ at basic pH, which is regarded as the preferred coagulant agent, enhances Pb^{2+} removal through adsorption and coprecipitation, as it forms a relatively stable precipitate [63]. Moreover, this is further supported by the fact that alkaline conditions favor complex polymerization allowing Pb^{2+} ions to form hydroxide complexes such as $Pb(OH)^+$, which are more readily adsorbed onto the negatively charged $Fe(OH)_3$ surface [45]. Similarly, Gong et al. [84] reported in their study that iron anode electrodes led to considerably higher selenium removal rates compared to aluminum; i.e., 79 % instead of 33 % respectively, during the electrocoagulation of food industry wastewater at 10 mA/cm^2 for 90 min. In the same way, Moussavi et al. [85] demonstrated that Fe-Fe electrode arrangement removed 87 % of cyanide from synthetic wastewater under 15 mA/cm^2 in 20 min, exceeding the 32 % removal achieved with Al-Fe arrangement. In general, the effectiveness of the electrode material depends on the specific EC application, as well as the composition and physicochemical properties of the treated wastewater, such as initial pH and eC, and most importantly, the target pollutant.

Interestingly, the EnC remains relatively constant across all three experiments, with the Fe/Fe electrodes showing a slightly lower EnC. It is therefore evident that the Fe/Fe electrode pair achieves the best results in both Pb^{2+} percentage removal and energy consumption, making it the most efficient configuration among the three options. This is particularly favorable, as it is also has the lowest cost [40,61].

3.3. Integrated electrocoagulation/electrochemical oxidation

Although Pb^{2+} can be effectively removed by EC process, PhOH removal did not provide encouraging results (data not shown here). Thus, the combined EC/EO process was tested with main objective to investigate the percentage removal of PhOH and Pb^{2+} under the specific experimental conditions as obtained from the optimization of EC process. Table 7 summarizes the experimental conditions of 3 experiments performed in two replicates using the integrated EC/EO process. All the results presented herein are the average values of the replicates. In Table 7 the two mentioned values of current densities were obtained due to the different surface areas of the anode electrodes; i.e., Fe and BDD, as given above in subsection 2.2.1.

The EC/EO unit operates in batch mode under constant current. It should be noted at this point that although the electrolysis time and experimental (or treatment) time are both adjusted by the recirculation flow rate, this should not be confused. The electrolysis time corresponds to the residence time of the solution in the electrolysis vessel, while the treatment time corresponds to the total hydraulic residence time in the pilot unit; i.e., the time required for the entire volume of feed solution (2.75 or 5 L) to pass through the system once. Two of the three experiments (Exp. No 20 and 21) were carried out with a synthetic, simulated solution and one (Exp. No 22) with a real SCWG wastewater (Table 3). Notably, Exp. No 22 was performed in two consecutive electrolysis cycles instead of a single cycle. It should also be taken into account that the concentration of lead ions in the mixed brine was negligible. Therefore, in Exp. No 22, the corresponding amount of $Pb(NO_3)_2$ was added to the feed solution to obtain the same initial Pb^{2+} concentration and to compare the results with those of previous experiments. Furthermore, the organic load of the brine, measured as TOC concentration, largely corresponds to other organic compounds such as formic acid, acetic acid, ethanol, methanol, resorcinol, glucose, sucrose, etc. rather than phenol. As such, the optimized parameters derived from synthetic wastewater experiments should be considered as indicative rather than universally applicable.

3.3.1. Total organic carbon, phenol and heavy metals concentration

The overall assessment of the combined EC/EO process in terms of PhOH degradation and mineralization as well as Pb^{2+} removal is summarized in Fig. 6. In the case of the synthetic feed solution (Exp. No 20 and 21), low current densities and short electrolysis times lead to an insignificant and rather limited process performance. However, doubling the current density from 32 to 64 mA/cm^2 and extending the electrolysis time from 9 to 66 min clearly favors the percentage removal of PhOH and TOC, reaching up to 38 % and 11 %, respectively. This positive effect is achieved by reducing the flow rate from 175 to 24 ml/

Table 6
EC experiments with different sacrificial anodes under the optimum operating conditions.

Exp. No	Electrodes Anode/ Cathode	Current Density (mA/ cm^2)	Electrolysis Time (min)	Initial pH	Pb^{2+} removal (%)	Energy Consumption (kWh/m^3)
17	Fe/Fe	10	9	10	88.5	0.88
18	Al/Fe	10	9	10	34.4	1.50
19	SS/Fe	10	9	10	18.2	1.12

Table 7
Main experimental conditions of the EC/EO process.

Exp. No	Current Density (mA/cm[b])	Flow Rate (ml/min)	Electrolysis Time (min)	Treatment Time (min)	Current (A)	Voltage (V)	Initial pH	Initial eC (mS/cm)	Initial PhOH (mg/L)	Initial Pb^{2+} (mg/L)
20	10/32[a]	175[b]	9	29	2.0	6.8[b]	11.3	3.78	239	7.5
21	20/64[a]	24[b]	66	208	4.0	9.3[b]	11.6	3.71	229	6.2
22	20/64[a]	24[b]	66/132[c]	115/230[c]	4.0	12.5[b]	8.6	3.32	411	6.4

[a] Fe anode/ BDD anode,
[b] Median values,
[c] 1st cycle/2nd cycle

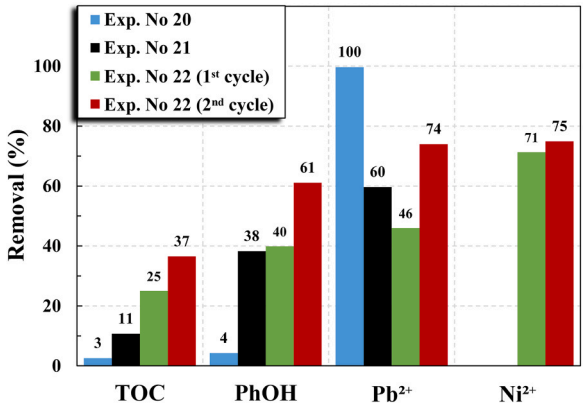

Fig. 6. Percentage removal of TOC, PhOH, Pb^{2+} and Ni^{2+} concentration after treatment with the EC/EO process.

min, which prolongs the contact time between the feed solution and the anode electrodes in the electrolysis vessel and increases the formation of strong hydroxyl radicals (•OH). Furthermore, it is well-established that CD regulates crucial parameters such as the coagulant dosage rate, bubble production rate and even the growth and size of flocs [62,65,66]. Consequently, an increase in CD promotes iron dissolution, which, according to Faraday's law, leads to greater production of ions (Fe^{2+} or Fe^{3+}) at the electrodes, resulting in higher pollutant removal rates by adsorption/settling and enhancing the overall efficiency of the EC/EO process [37,51]. These results are in agreement with those reported by Liu et al. (2024) [86], where PhOH mineralization levels ranging from 46 % to 53 % were observed, after 60 min of EO using a BDD anode at a CD of 6.46 mA/cm^2, treating synthetic wastewater with a lower initial PhOH concentration of 50 mg/L.

In contrast, the results of the inorganic decontamination of the synthetic feed solution show that the complete removal of Pb^{2+} is achieved with a lower current density and a higher flow rate, which correlates with a short electrolysis time (Exp. No 20). These findings are consistent with the results of the previously described EC experiments and are also supported by literature reports. For instance, Khosa et al. [87] reported 96 % Pb^{2+} removal under almost similar conditions to those in the current study, i.e., pH 9 and t = 10 min, while Thakur et al. [88] achieved 92 % Pb^{2+} removal at pH 7 after 20 min with current density 10 mA/cm^2; both studies involved the treatment of synthetic wastewater using Fe-Fe electrodes.

Fig. 6 also shows that the combined EC/EO process works well even when treating a real saline concentrated feed solution (Exp. No 22), as the efficiency remains at a rather high level after the second electrolysis cycle; i.e., 37 % mineralization and 61 % degradation of PhOH, respectively. Moreover, the overall performance after the second sequential electrolysis cycle increases compared to the performance after the first cycle, as mostly expected. In particular, TOC and PhOH removal increases by 48 % and 53 % respectively, while Pb^{2+} removal increases by 61 %, reaching 74 %. These percentage removals are quite impressive, considering that the organic load of the real wastewater (Exp. No 22) is about 5 times higher than in the synthetic feed solution (Exp. No 20 and 21); i.e., 822 mg/L instead of 170 mg/L TOC. Similarly, the initial PhOH concentration is approx. 2 times as high; i.e., 411 mg/L compared to 229 mg/L PhOH. In related studies involving combined process EC/EO (EC followed by EO) applied to real wastewater, Linares et al. [74] reported 75 % TOC removal using Cu and BDD anodes after 6 h of treatment at 17 mA/cm^2 for wastewater from a soft drink industry, whereas Gengec et al. [75] using Al and BDD anodes noted 47 % mineralization of carbon plant wastewater within 180 min at pH 7.2 and 25 mA/cm^2.

Apart from this, 75 % removal of Ni^{2+} is achieved in the same experiment, proving the great effectiveness of the integrated process in removing the actual inorganic load of the brine (expressed as heavy metals). Ni^{2+} removal efficiencies in the same range (94 % and 87 %) have also been reported in the literature by Al Sannag et al. [45], who treated a real wastewater from metal plating by EC process with Fe anode at pH 10.7 for 60 min under a current density of 4 mA/cm^2 and by Harahap et al. [53], who achieved comparable results using Al electrodes after 45 min of treating artificial mining industry wastewater at 9.6 pH and 10 mA/cm^2.

3.3.2. Kinetics

A kinetic analysis of PhOH and TOC removal was also performed, showing that the degradation and mineralization rates of PhOH follow pseudo-first order reaction kinetics, with the concentration of PhOH and TOC, respectively, at time t being proportional to the initial concentration and treatment time according to Eq. (11).

$$C_t = C_o \bullet e^{-kt} \quad (11)$$

where, C_o is the initial PhOH or TOC concentration (mg/L), C_t is the corresponding PhOH or TOC concentration at treatment time t (h) and k is the apparent first order rate constant (h^{-1}). The rate constants were estimated from the slope of the straight line resulting from the plots of ln C_t/C_o versus time, based on Eq. (12).

$$\ln \frac{c_t}{c_o} = -kt \quad (12)$$

The reaction kinetics of PhOH degradation and the mechanisms of mineralization of organic matter for the two experiments performed at the same current density and flow rate (Exp. No 21 and 22) are presented in Fig. S3 and S4 in the Supplement. It is shown that the reduction in PhOH and TOC concentrations is more rapid during the first hour and becomes slower toward the end of the treatment in both experiments. The apparent rate constants k and the coefficients of determination R^2 of

Table 8
First order kinetic constants and coefficients of determination of PhOH and TOC removal during the EC/EO process.

Exp. No	PhOH		TOC	
	k (min^{-1})	R^2	k (min^{-1})	R^2
21	24.5×10^{-4}	0.944	5.6×10^{-4}	0.943
22	43.3×10^{-4}	0.921	22.2×10^{-4}	0.753

these two experiments with synthetic and real wastewater, respectively, are listed in Table 8. It can be observed that the degradation of PhOH in the case of the real brine is about 1.8 times faster than in the simulated solution. In contrast, the rate constants of mineralization of PhOH and other organics are either an order of magnitude lower (Exp. No 21) or with a rather low coefficient of determination (Exp. No 22). Likewise, Patel et al. [34] and Kumar et al. [47] confirmed that the electrocoagulation process during COD removal from greywater and paper industry wastewater respectively, followed pseudo-first-order kinetics. Notably, the kinetic rate constant reported by Kumar et al. [47] was of the same order of magnitude; i.e., 39.7 min^{-1}, as that observed in the experiment with real brine. Foaming was observed in the real brine from the beginning of the experiment, probably due to the physicochemical properties of the concentrated mixed saline solution. This foam, which is an indication of potential system fouling, became heavier and more intense as the treatment duration increased and can be attributed to the formation of volatile organic compounds and CO_2 during the mineralization of the brine. The foaming evolution is shown in Fig. S5 of the Supplement.

3.3.3. Energy consumption and total suspended solids

To evaluate the process, energy consumption (EnC), considered as the kWh consumed per m^3 of wastewater, is calculated according to Eq. (12). Fig. 7 shows the EnC and TSS concentration in experiments using the combined EC/EO method. The EnC values in this study are between 1 and 70 kWh/m^3 within the range of relevant (mostly EC) applications reported in the literature, typically varying from 0.15 to 100 kWh/m^3 [67,68]. For example, Fajardo et al. [46] reported a EnC of 34 kWh/m^3 for the treatment of a real olive mill effluent and the removal of 21 % COD and 72 % total phenolic content, applying 25 mA/cm^2 CD and 180 min ET, while Akkaya [89] achieved an EnC of 31.2 kWh/m^3 for the removal of 96 % COD and 94 % PhOH from petroleum wastewater under optimal experimental conditions (22 mA/cm^2 and 39 min). Other EC studies, such as those by Jallouli et al. [43], Esfandyari et al. [90] and Tezcan et al. [91] reported similar EnC values of 33, 75 and 101 kWh/m^3 respectively, for attaining 80–85 % COD reduction from industrial and hospital wastewaters. Concerning previous works on the combined EC/EO process, equally comparable EnC values were recorded by the researchers in various conditions. Specifically, 76 kWh/m^3 was reported for 45 % TOC and 49 % COD removal from cardboard plant wastewater after 180 min [75], 18 kWh/m^3 was obtained for complete COD removal from tannery wastewater after 50 min [76] and a range of 21–50 kWh/m^3 was noted for 72–85 % nitrate reduction from nitrate-polluted groundwaters after 90–210 min [77]. Increasing the current density (Exp. No 21) and extending the treatment time (2nd cycle of Exp. No 22) leads to an increase in the EnC value. Moreover, the relatively low EnC value (1.3 kWh/m^3) required for the complete removal of Pb^{2+} from the synthetic feed solution (Exp. No 20) confirms the very high efficiency of the combined EC/EO process and the very good performance of the laboratory pilot experiment under the near-optimal experimental conditions.

The samples for measuring the TSS concentration were taken from the sedimentation vessel at the end of the treatment period. The TSS concentration at the end of the two experiments with synthetic feed solution (Exp. No 20 and 21) shows exactly the same amount of sludge production (about 180 mg/L), which is mainly due to the deterioration of Fe anode electrode through oxidation that gradually develops with the treatment time. The Fe electrode deterioration can be observed in Fig. S5c of the Supplement. In general, the TSS concentration decreases with lower current densities and longer electrolysis times.

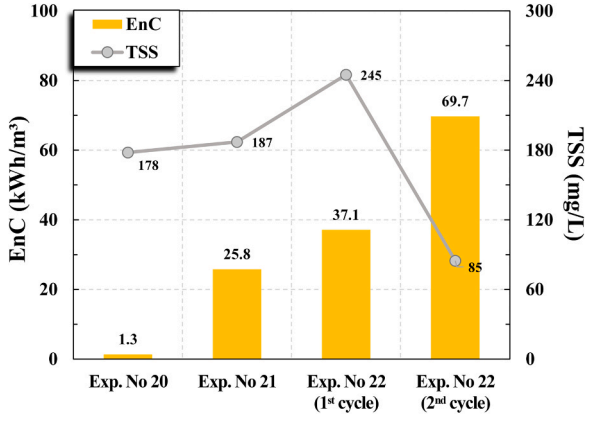

Fig. 7. EnC and TSS concentration after treatment with the EC/EO process.

3.3.4. Turbidity

Finally, turbidity measurements were carried out on samples taken from the supernatant of the sedimentation vessel during the experiments. The results are shown in Fig. 8 as a function of normalized treatment time to facilitate comparison. The conclusion is that the high Pb^{2+} removal is consistent with the turbidity values in the case of the low current density experiment (Exp. No 20), as the turbidity decreases with time and reaches very low values (4 NTU) at the end of the experiment. This indicates effective settling of the coagulants, resulting in a clearer supernatant liquid. However, in the other case (Exp. No 21), the turbidity increases with the treatment time, probably due to the formation of Fe and Pb complexes, which seem to act more as an inhibitory factor. As stated in a previous publication [63], the complexation mechanism involves heavy metals acting as ligands, forming bonds with the hydrous groups of the coagulant floc (primarily $Fe(OH)_3$ at this specific pH), leading to the formation of surface complexes. The presence of this type of complexes is confirmed by the overall spectra of the samples taken during the treatment (data not shown), where interferences are observed during the analysis. On the other hand, although the turbidity remains relatively stable (with small variations) when tested with real brine (Exp. No 22), the values are significantly higher, averaging approx. 155 NTU.

4. Conclusions

The convenient application of electric current instead of chemicals proves to be very effective in the combined removal of heavy metals (lead) and the degradation/mineralization of organic matter (PhOH) in saline waters, as they occur in the treatment of various biomasses by SCWG. The combined process of Electrocoagulation and Electrochemical Oxidation in a single unit, consisting of pairs of sacrificial Fe and BDD anodes, offers distinct advantages for large-scale applications such as versatility, energy efficiency, amenability of automation, the

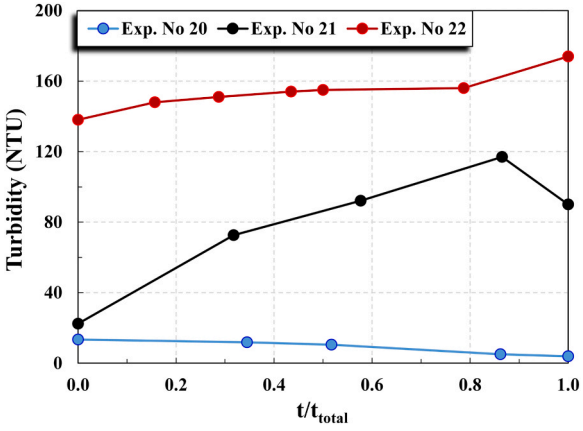

Fig. 8. Temporal variation of turbidity during treatment with the EC/EO process.

possibility to avoid the addition of chemicals, and safety as they operate under mild conditions. In experiments with synthetic simulated wastewater in an EC/EO laboratory pilot unit with two pairs of metal electrodes (Fe/Fe and BDD/SS) arranged in parallel and operated at constant current, almost complete (> 99 %) removal of Pb^{2+} at a current density of 32 mA/cm^2 and an electrolysis time of 9 min was achieved. Experiments with real SCWG wastewater showed an even higher efficiency concerning PhOH degradation and mineralization rates. In particular, the removal of PhOH and TOC reached 61 % and 37 %, respectively, at a current density of 64 mA/cm^2 and after two consecutive electrolysis cycles, corresponding to an electrolysis time of 132 min. Under these optimal experimental conditions, approx. 75 % of the Pb^{2+} and Ni^{2+} were removed, making the combined EC/EO process very efficient. From an energy perspective, the very low energy consumption (1.3 kWh/m^3) during the complete removal of Pb^{2+} ions from a synthetic SCWG brine indicates the cost-effectiveness of the combined EC/EO process. Meanwhile, the energy demand of 69.7 kWh/m^3 required to achieve high-level inorganic and organic decontamination from a real SCWG brine is comparable to values (up to 100 kWh/m^3) commonly reported in other electrocoagulation studies, although a direct comparison may not be entirely appropriate due to differences in wastewater composition and treatment goals. The PhOH degradation reaction also follows pseudo-first order kinetics and the rate constant for the real brine is estimated to be 1.8 times larger than that for the simulated one. Finally, the rather high concentration of TSS, which correlates with sludge production during sedimentation, is mainly due to the gradual decomposition of the Fe electrodes during electrolysis. The latter seems to favor the formation of Fe and Pb complexes during the treatment period, which probably acts as an inhibiting factor in the removal of Pb^{2+}.

CRediT authorship contribution statement

Vasilis C. Sarasidis: Writing – original draft, Visualization, Methodology, Investigation, Formal analysis, Data curation. **Julian Dutzi:** Writing – original draft, Visualization, Validation, Investigation, Formal analysis, Data curation, Conceptualization. **Panagiota N. Petsi:** Methodology, Investigation. **Konstantinos V. Plakas:** Writing – review & editing, Supervision, Methodology, Funding acquisition, Conceptualization. **Nikolaos Boukis:** Writing – review & editing, Validation, Resources, Methodology, Funding acquisition, Conceptualization. **Jörg Sauer:** Writing – review & editing, Validation, Supervision.

Declaration of Competing Interest

The authors declare that they have no known competing financial interests or personal relationships that could have appeared to influence the work reported in this paper.

Acknowledgments

The work was financially supported by the project: CERESiS – ContaminatEd land Remediation through Energy crops for Soil improvement to liquid biofuel Strategies, funded by the European Union's Horizon 2020 research and innovation program under grant agreement No. 101006717..

Appendix A. Supporting information

Supplementary data associated with this article can be found in the online version at doi:10.1016/j.jece.2025.118491.

Data availability

Data will be made available on request.

References

[1] A. Kruse, E. Dinjus, Hot compressed water as reaction medium and reactant, Prop. Synth. React. J. Supercrit. Fluids 39 (2007) 362–380, https://doi.org/10.1016/j.supflu.2006.03.016.
[2] A. Kruse, Supercritical water gasification, Biofuels Bioprod. Bioref. 2 (2008) 415–437, https://doi.org/10.1002/bbb.93.
[3] A. Loppinet-Serani, C. Aymonier, F. Cansell, Current and foreseeable applications of supercritical water for energy and the environment, ChemSusChem 1 (2008) 486–503, https://doi.org/10.1002/cssc.200700167.
[4] A.A. Galkin, V.V. Lunin, Subcritical and supercritical water: a universal medium for chemical reactions, Russ. Chem. Rev. 74 (2005) 21–35, https://doi.org/10.1070/RC2005v074n01ABEH001167.
[5] S. Wang, D. Xu, Y. Guo, X. Tang, Y. Wang, J. Zhang, H. Ma, L. Qian, Y. Li, Supercritical water processing technologies for environment, energy and nanomaterial applications, Springer, Singapore, Singapore, 2020, https://doi.org/10.1007/978-981-13-9326-6.
[6] J.A. Okolie, R. Rana, S. Nanda, A.K. Dalai, J.A. Kozinski, Supercritical water gasification of biomass: a state-of-the-art review of process parameters, reaction mechanisms and catalysis, Sustain. Energy Fuels 3 (2019) 578–598, https://doi.org/10.1039/c8se00565f.
[7] M.H. Waldner, F. Vogel, Renewable production of methane from woody biomass by catalytic hydro-thermal gasification, Ind. Eng. Chem. Res. 44 (2005) 4543–4551, https://doi.org/10.1021/ie050161h.
[8] J. Dutzi, N. Boukis, J. Sauer, Process effluent recycling in the supercritical water gasification of dry biomass, Processes 11 (3) (2023) 797, https://doi.org/10.3390/pr11030797.
[9] J. Dutzi, A.A. Vadarlis, N. Boukis, J. Sauer, Development and parametrization of a novel reactor concept for the supercritical water gasification process, Ind. Eng. Chem. Res. 64 (2025) 9500–9517, https://doi.org/10.1021/acs.iecr.4c04267.
[10] J. Dutzi, A.A. Vadarlis, N. Boukis, J. Sauer, Comparison of experimental results with thermodynamic equilibrium simulations of supercritical water gasification of concentrated ethanol solutions with focus on water splitting, Ind. Eng. Chem. Res. 62 (2023) 12501–12512, https://doi.org/10.1021/acs.iecr.3c01595.
[11] N. Boukis, V. Diem, E. Dinjus, G. Franz, H. Schmieder, Reforming of methanol at supercritical water conditions. First experimental results, in: AIDIC Conference Series, 5, 2002, pp. 65–70.
[12] J. Dutzi, N. Boukis, J. Sauer, Supercritical water gasification of heavy metal contaminated plants with focus on separation of heavy metal contaminants, Biomass. Bioenergy 182 (2024), https://doi.org/10.1016/j.biombioe.2024.107059.
[13] J. Dutzi, I.K. Stoll, N. Boukis, J. Sauer, Screening of ten different plants in the process of supercritical water gasification, Sustain. Chem. Environ. 5 (2024) 100062, https://doi.org/10.1016/j.scenv.2024.100062.
[14] N. Boukis, I.K. Stoll, J. Sauer, J. Fischer, R. Kansy, Separation of salts during the gasification of spent grain in supercritical water, in: 25th European Biomass Conference and Exhibition, Stockholm, Sweden, 2017.
[15] N. Boukis, I.K. Stoll, Gasification of biomass in supercritical water, challenges for the process design–lessons learned from the operation experience of the first dedicated pilot plant, Processes 9 (2021) 1–17, https://doi.org/10.3390/pr9030455.
[16] K. Heeley, R.L. Orozco, L.E. Macaskie, J. Love, B. Al-Duri, Supercritical water gasification of microalgal biomass for hydrogen production-A review, Int. J. Hydrog. Energy 49 (2024) 310–336, https://doi.org/10.1016/j.ijhydene.2023.08.081.
[17] M. Schubert, J.W. Regler, F. Vogel, Continuous salt precipitation and separation from supercritical water. Part 1: type 1 salts, J. Supercrit. Fluids 52 (1) (2010) 99–112, https://doi.org/10.1016/j.supflu.2009.10.002.
[18] M. Hodes, P.A. Marrone, G.T. Hong, K.A. Smith, J.W. Tester, Salt precipitation and scale control in supercritical water oxidation - part A: fundamentals and research, J. Supercrit. Fluids 29 (2004) 265–288, https://doi.org/10.1016/S0896-8446(03)00093-7.
[19] L. Lu, S. Liu, Z. Fang, Z. Peng, W. Cao, H. Jin, Y. Chen, L. Guo, Mechanism of salt deposition, nucleation and separation in the supercritical water gasification of black liquor, Chem. Eng. J. 506 (2025) 159914, https://doi.org/10.1016/j.cej.2025.159914.
[20] N. Boukis, U. Galla, Verfahren zur hydrothermalen Vergasung von Biomasse in überkritischem Wasser, DE 10 2006 044 116 B3, 2008.
[21] P. D'Jesús, Die Vergasung von realer Biomasse in überkritischem Wasser, Dissertation, Universität Karlsruhe, 2007.
[22] C. Zörb, M. Senbayram, E. Peiter, Potassium in agriculture – status and perspectives, J. Plant Physiol. 171 (2014) 656–669, https://doi.org/10.1016/j.jplph.2013.08.008.
[23] D. Cordell, S. White, Peak phosphorus: clarifying the key issues of a vigorous debate about long-term phosphorus security, Sustainability 3 (2011) 2027–2049, https://doi.org/10.3390/su3102027.
[24] CERESiS, CERESiS, (2024). ⟨https://ceresis.eu/⟩ (accessed March 14, 2024).
[25] V. Kumar, S.K. Dwivedi, S. Oh, A critical review on lead removal from industrial wastewater: recent advances and future outlook, J. Water Proc. Eng. 45 (2022) 102518, https://doi.org/10.1016/j.jwpe.2021.102518.
[26] H.K. Shon, S. Vigneswaran, S.A. Snyder, Effluent organic matter (EfOM) in wastewater: constituents, effects, and treatment, Crit. Rev. Environ. Sci. Technol. 36 (2006) 327–374, https://doi.org/10.1080/10643380600580011.
[27] J. Iniesta, P.A. Michaud, M. Panizza, G. Cerisola, A. Aldaz, Ch Comninellis, Electrochemical oxidation of phenol at boron-doped diamond electrode,

Electrochim. Acta 46 (2001) 3573–3578, https://doi.org/10.1016/S0013-4686(01)00630-2.
[28] D.T. Moussa, M.H. El-Naas, M. Nasser, M.J. Al-Marri, A comprehensive review of electrocoagulation for water treatment: potentials and challenges, J. Environ. Manag. 186 (2017) 24–41, https://doi.org/10.1016/j.jenvman.2016.10.032.
[29] I. García, L.F. Castaneda, J.L. Nava, O. Coreno, Continuous electrocoagulation-flocculation-sedimentation process to remove arsenic, fluoride, and hydrated silica from drinking water, J. Water Process Eng. 69 (2025) 106571, https://doi.org/10.1016/j.jwpe.2024.106571.
[30] J.-Q. Jiang, N. Graham, C. Andre, G.H. Kelsall, N. Brandon, Laboratory study of electro-coagulation–flotation for water treatment, Water Res. 36 (2002) 4064–4078, https://doi.org/10.1016/S0043-1354(02)00118-5.
[31] K.S. Hashim, I.A. Idowu, N. Jasim, R. Al Khaddar, A. Shaw, et al., Removal of phosphate from river water using a new baffle plates electrochemical reactor, MethodsX 5 (2018) 1413–1418, https://doi.org/10.1016/j.mex.2018.10.024.
[32] M.R. Al-Kilani, K. Bani-Melhem, The performance of electrocoagulation process for decolorization and COD removal of highly colored real grey water under variable operating conditions, Desalin. Water Treat. 321 (2005) 100924, https://doi.org/10.1016/j.dwt.2024.100924.
[33] K. Bani-Melhem, M. Al-Shannag, D. Alrousan, S. Al-Kofahi, Z. Al-Qodah, M.R. Al-Kilani, Impact of soluble COD on grey water treatment by electrocoagulation technique, Desalin. Water Treat. 89 (2017) 101–110, https://doi.org/10.5004/dwt.2017.21379.
[34] P. Patel, S. Gupta, P. Mondal, Electrocoagulation process for greywater treatment: statistical modeling, optimization, cost analysis and sludge management, Sep. Purif. Technol. 296 (2022) 121327, https://doi.org/10.1016/j.seppur.2022.121327.
[35] N. Najid, B. Gourich, S. Kouzbour, M.C. Ncibi, A. El Midaoui, Impact of saline water matrix on the removal of boron using electrocoagulation process: unveiling performance, removal mechanism, and cost-energy evaluation, Chem. Eng. Process. Process. Intensif. 207 (2025) 110069, https://doi.org/10.1016/j.cep.2024.110069.
[36] F.Y. AlJaberi, S.A. Ahmed, H.F. Makki, Electrocoagulation treatment of high saline oily wastewater: evaluation and optimization, Heliyon 6 (6) (2020) e03988, https://doi.org/10.1016/j.heliyon.2020.e03988.
[37] A.A. Al-Raad, M.M. Hanafiah, A.S. Naje, M.A. Ajeel, A.O. Basheer, et al., Treatment of saline water using electrocoagulation with combined electrical connection of electrodes, Processes 7 (2019) 242, https://doi.org/10.3390/pr7050242.
[38] A.A. Al-Raad, M.M. Hanafiah, A.S. Naje, M.A. Ajeel, Optimized parameters of the electrocoagulation process using a novel reactor with rotating anode for saline water treatment, Environ. Pollut. 265 (2020) 115049, https://doi.org/10.1016/j.envpol.2020.115049.
[39] S.P. Azerrad, M. Isaacs, C.G. Dosoretz, Integrated treatment of reverse osmosis brines coupling electrocoagulation with advanced oxidation processes, Chem. Eng. J. 356 (2019) 771–780, https://doi.org/10.1016/j.cej.2018.09.068.
[40] M. Kobya, O. Taner Can, M. Bayramoglu, Treatment of textile wastewaters by electrocoagulation using iron and aluminum electrodes, J. Hazard. Mater. B100 (2003) 163–178, https://doi.org/10.1016/S0304-3894(03)00102-X.
[41] E. Yuksel, M. Eyvaz, E. Gurbulak, Electrochemical treatment of colour index reactive orange 84 and textile wastewater by using stainless steel and iron electrodes, Environ. Prog. Sust. Energy 32 (1) (2013) 60–68, https://doi.org/10.1002/ep.10601.
[42] E. Bazrafshan, M.R. Alipour, A.H. Mahvi, Textile wastewater treatment by application of combined chemical coagulation, electrocoagulation and adsorption processes, Desalin. Water Treat. 57 (20) (2016) 9203–9215, https://doi.org/10.1080/19443994.2015.1027960.
[43] S. Jallouli, A. Wali, A. Buonerba, T. Zarra, V. Belgiorno, V. Naddeo, M. Ksibi, Efficient and sustainable treatment of tannery wastewater by a sequential electrocoagulation-UV photolytic process, J. Water Process Eng. 38 (2020) 101642, https://doi.org/10.1016/j.jwpe.2020.101642.
[44] A.D. Villalobos-Lara, F. Alvarez, Z. Gamino-Arroyo, R. Navarro, J.M. Peralta-Hernandez, R. Fuentes, T. Perez, Electrocoagulation treatment of industrial tannery wastewater employing a modified rotating cylinder electrode reactor, Chemosphere 264 (2021) 128491, https://doi.org/10.1016/j.chemosphere.2020.128491.
[45] M. Al-Shannag, Z. Al-Qodah, K. Bani-Melhem, M. Rasool Qtaishat, M. Alkasrawi, Heavy metal ions removal from metal plating wastewater using electrocoagulation: kinetic study and process performance, Chem. Eng. J. 260 (2015) 749–756, https://doi.org/10.1016/j.cej.2014.09.035.
[46] A.S. Fajardo, R.F. Rodrigues, R.C. Martins, L.M. Castro, R.M. Quinta-Ferreira, Phenolic wastewaters treatment by electrocoagulation process using Zn anode, Chem. Eng. J. 275 (2015) 331–341, https://doi.org/10.1016/j.cej.2015.03.116.
[47] D. Kumar, C. Sharma, Paper industry wastewater treatment by electrocoagulation and aspect of sludge management, J. Clean. Prod. 360 (2022) 131970, https://doi.org/10.1016/j.jclepro.2022.131970.
[48] A. Strugała-Wilczek, Ł. Jałowiecki, M. Szul, J. Borgulat, G. Płaza, K. Stanczyk, A hybrid system based on the combination of adsorption, electrocoagulation, and wetland treatment for the effective remediation of industrial wastewater from underground coal gasification (UCG, J. Environ. Manag 371 (2024) 123180, https://doi.org/10.1016/j.jenvman.2024.123180.
[49] I. Linares-Hernández, C. Barrera-Díaz, B. Bilyeu, P. Juárez-GarcíaRojas, E. Campos-Medina, A combined electrocoagulation–electrooxidation treatment for industrial wastewater, J. Hazard. Mater. 175 (1–3) (2010) 688–694, https://doi.org/10.1016/j.jhazmat.2009.10.064.
[50] D. Syam Babu, T.S. Anantha Singh, P.V. Nidheesh, M. Suresh Kumar, Industrial wastewater treatment by electrocoagulation process, Sep. Purif. Technol. 55 (17) (2020) 3195–3227, https://doi.org/10.1080/01496395.2019.1671866.
[51] B.K. Nandi, S. Patel, Effects of operational parameters on the removal of brilliant green dye from aqueous solutions by electrocoagulation, Arab. J. Chem. 10 (2017) S2961–S2968, https://doi.org/10.1016/j.arabjc.2013.11.032.
[52] S. Zodi, B. Merzouk, O. Potier, F. Lapicque, J.-P. Lecler, Direct red 81 dye removal by a continuous flow electrocoagulation/flotation reactor, Sep. Purif. Technol. 108 (2013) 215–222, https://doi.org/10.1016/j.seppur.2013.01.052.
[53] M.G. Harahap, M.S. Abfertiawan, M. Syafila, M. Handajani, T.H. Gultom, Electrocoagulation for nickel, chromium, and iron removal from mine water using aluminum electrodes, Heliyon 10 (2024) e40784, https://doi.org/10.1016/j.heliyon.2024.e40784.
[54] P. Gao, X. Chen, F. Shen, G. Chen, Removal of chromium(VI) from wastewater by combined electrocoagulation–electroflotation without a filter, Sep. Purif. Technol. 43 (2005) 117–123, https://doi.org/10.1016/j.seppur.2004.10.008.
[55] J.R. Parga, D.L. Cocke, J.L. Valenzuela, J.A. Gomes, M. Kesmez, G. Irwin, H. Moreno, M. Weir, Arsenic removal via electrocoagulation from heavy metal contaminated groundwater in La Comarca Lagunera Mexico, J. Hazard. Mater. 124 (1–3) (2005) 247–254, https://doi.org/10.1016/j.jhazmat.2005.05.017.
[56] M.M.S.G. Eiband, K.C. de, A. Trindade, K. Gama, J. Vieira de Melo, C.A. Martínez-Huitle, S. Ferro, Elimination of Pb^{2+} through electrocoagulation: applicability of adsorptive stripping voltammetry for monitoring the lead concentration during its elimination, J. Electroanal. Chem. 717-718 (2014) 213–218, https://doi.org/10.1016/j.jelechem.2014.01.032.
[57] F. Boysan, A. Çavunt, Investigation of bisphenol A removal using peroxy electrocoagulation method, Desalin. Water Treat. 222 (2021) 426–433, https://doi.org/10.5004/dwt.2021.27423.
[58] H.A. Moreno-Casillas, D.L. Cocke, J.A.G. Gomes, P. Morkovsky, J.R. Parga, E. Peterson, Electrocoagulation mechanism for COD removal, Sep. Purif. Technol. 56 (2007) 204–211, https://doi.org/10.1016/j.seppur.2007.01.031.
[59] A. El-Ghenymy, M. Alsheyab, A. Khodary, I. Sires, A. Abdel-Wahab, Corrosion behavior of pure titanium anodes in saline medium and their performance for humic acid removal by electrocoagulation, Chemosphere 246 (2020) 125674, https://doi.org/10.1016/j.chemosphere.2019.125674.
[60] D. Xu, Y. Li, L. Yin, Y. Ji, J. Niu, Y. Yu, Electrochemical removal of nitrate in industrial wastewater, Front. Environ. Sci. Eng. 12 (9) (2018), https://doi.org/10.1007/s11783-018-1033-z.
[61] J.N. Hakizimana, B. Gourich, M. Chafi, Y. Stiriba, C. Vial, P. Drogui, J. Naja, Electrocoagulation process in water treatment: a review of electrocoagulation modeling approaches, Desalination 404 (2017) 1–21, https://doi.org/10.1016/j.desal.2016.10.011.
[62] V. Khandegar, A.K. Saroha, Electrocoagulation for the treatment of textile industry effluent – a review, J. Environ. Manag. 128 (2013) 949–963, https://doi.org/10.1016/j.jenvman.2013.06.04.
[63] S. Garcia-Segura, M.M.S.G. Eiband, J.Vieira de Melo, C.A. Martínez-Huitle, Electrocoagulation and advanced electrocoagulation processes: a general review about the fundamentals, emerging applications and its association with other technologies, J. Electroanal. Chem. 801 (2017) 267–299, https://doi.org/10.1016/j.jelechem.2017.07.047.
[64] P.V. Nidheesh, J. Scaria, D.S. Babu, M.S. Kumar, An overview on combined electrocoagulation-degradation processes for the effective treatment of water and wastewater, Chemosphere 263 (2021) 127907, https://doi.org/10.1016/j.chemosphere.2020.127907.
[65] R. Alam, S.U. Khan, M. Usman, M. Asif, I.H. Farooqi, A critical review on treatment of saline wastewater with emphasis on electrochemical based approaches, Process Saf. Environ. Prot. 158 (2022) 625–643, https://doi.org/10.1016/j.psep.2021.11.054.
[66] S. Boinpally, A. Kolla, J. Kainthola, R. Kodali, J. Vemuri, A state-of-the-art review of the electrocoagulation technology for wastewater treatment, Water Cycle 4 (2023) 26–36, https://doi.org/10.1016/j.watcyc.2023.01.001.
[67] P.T.P. Aryanti, F.A. Nugroho, C. Phalakornkule, A. Kadier, Energy efficiency in electrocoagulation processes for sustainable water and wastewater treatment, J. Environ. Chem. Eng. 12 (6) (2024) 114124, https://doi.org/10.1016/j.jece.2024.114124.
[68] S.K. Patel, S.C. Shukla, B.R. Natarajan, P. Asaithambi, H.K. Dwivedi, et al., State of the art review for industrial wastewater treatment by electrocoagulation process: mechanism, cost and sludge analysis, Desalin. Water Treat. 321 (2025) 100915, https://doi.org/10.1016/j.dwt.2024.100915.
[69] C.A. Martínez-Huitle, M. Panizza, Electrochemical oxidation of organic pollutants for wastewater treatment, Curr. Opin. Electrochem. 11 (2018) 62–71, https://doi.org/10.1016/j.coelec.2018.07.010.
[70] I. Sirés, E. Brillas, M.A. Oturan, M.A. Rodrigo, M. Panizza, Electrochemical advanced oxidation processes: today and tomorrow. A review, Environ. Sci. Pollut. Res. 21 (2014) 8336–8367, https://doi.org/10.1007/s11356-014-2783-1.
[71] S. Garcia-Segura, J.D. Ocon, M.N. Chong, Electrochemical oxidation remediation of real wastewater effluents – a review, Process. Saf. Environ. Prot. 113 (2018) 48–67, https://doi.org/10.1016/j.psep.2017.09.014.
[72] C.A. Martínez-Huitle, S. Ferro, Electrochemical oxidation of organic pollutants for the wastewater treatment: direct and indirect processes, Chem. Soc. Rev. 35 (2006) 1324–1340, https://doi.org/10.1039/B517632H.
[73] E. Mostafa, P. Reinsberg, S. Garcia-Segura, H. Baltruschat, Chlorine species evolution during electrochlorination on boron-doped diamond anodes: in-situ electrogeneration of Cl_2, Cl_2O and ClO_2, Electrochim. Acta 281 (2018) 831–840, https://doi.org/10.1016/j.electacta.2018.05.099.

[74] I. Linares-Hernández, C. Barrera-Díaz, M. Valdés Cerecero, P.T. Almazán Sánchez, M. Castañeda Juárez, V. Lugo Lugo, Soft drink wastewater treatment by electrocoagulation–electrooxidation processes, Environ. Technol. 38 (4) (2016) 433–442, https://doi.org/10.1080/09593330.2016.1196740.
[75] E. Gengec, Treatment of highly toxic cardboard plant wastewater by a combination of electrocoagulation and electrooxidation processes, Ecotoxicol. Environ. Saf. 145 (2017) 184–192, https://doi.org/10.1016/j.ecoenv.2017.07.032.
[76] G. Azarian, M. Miri, D. Nematollahi, Combined electrocoagulation/electrooxidation process for the COD removal and recovery of tannery industry wastewater, Environ. Prog. Sustain. Energy 37 (2) (2018), https://doi.org/10.1002/ep.12711.
[77] A.K. Benekos, M. Tsigara, S. Zacharakis, I.-E. Triantaphyllidou, A. G. Tekerlekopoulou, A. Katsaounis, D.V. Vayenas, Combined electrocoagulation and electrochemical oxidation treatment for groundwater denitrification, J. Environ. Manag. 285 (2021) 112068, https://doi.org/10.1016/j.jenvman.2021.112068.
[78] D.C. Montgomery. Introduction to Statistical Quality Control, 8th Edition, Wiley, 2019. ISBN: 978-1-119-39930-8.
[79] Y. Hu, M. Gong, X. Xing, H. Wang, Y. Zeng, C.C. Xu, Supercritical water gasification of biomass model compounds: a review, Renew. Sust. Energ. Rev. 118 (2020) 109529, https://doi.org/10.1016/j.rser.2019.109529.
[80] H. Babich, D.L. Davis, Phenol: a review of environmental and health risks, Regul. Toxicol. Pharm. 1 (1981) 90–109, https://doi.org/10.1016/0273-2300(81)90071-4.
[81] B.S. Lynch, E.S. Delzell, D.H. Bechtel, Toxicology review and risk assessment of resorcinol: thyroid effects, Regul. Toxicol. Pharm. 36 (2002) 198–210, https://doi.org/10.1006/rtph.2002.1585.
[82] E. Gasafi, M.Y. Reinecke, A. Kruse, L. Schebek, Economic analysis of sewage sludge gasification in supercritical water for hydrogen production, Biomass. Bioenergy 32 (2008) 1085–1096, https://doi.org/10.1016/j.biombioe.2008.02.021.
[83] L.E. Sommers, Chemical composition of sewage sludges and analysis of their potential use as fertilizers, J. Environ. Qual. 6 (1977) 225–232, https://doi.org/10.2134/jeq1977.00472425000600020026x.
[84] C. Gong, J. Zhang, X. Ren, C. He, J. Han, Z. Zhang, A comparative study of electrocoagulation treatment with iron, aluminum and zinc electrodes for selenium removal from flour production wastewater, Chemosphere 303 (2022) 135249, https://doi.org/10.1016/j.chemosphere.2022.135249.
[85] G. Moussavi, F. Majidi, F.M. Farzadkia, The influence of operational parameters on elimination of cyanide from wastewater using the electrocoagulation process, Desalination 280 (2011) 127–133, https://doi.org/10.1016/j.desal.2011.06.052.
[86] R. Liu, M. Ouyang, S. Chen, S. Wang, C. Liu, C. Zhang, H. Wu, The peculiar role of iodides and formation of iodinated oligomer byproducts upon phenol mineralization with boron-doped diamond anode, Chem. Eng. J. 501 (2024) 157517, https://doi.org/10.1016/j.desal.2011.06.052.
[87] M.K. Khosa, M.A. Jamal, A. Hussain, M. Muneer, K.M. Zia, S. Hafeez, Efficiency of aluminum and iron electrodes for the removal of heavy metals [(Ni (II), Pb (II), Cd (II)] by electrocoagulation method, J. Korean Chem. Soc. 57 (3) (2013), https://doi.org/10.5012/jkcs.2013.57.3.316.
[88] L.S. Thakur, R. Baghel, A. Sharma, S. Sharma, S. Verma, H. Parmar, A.K. Varma, P. Mondal, Simultaneous removal of lead, chromium and cadmium from synthetic water by electrocoagulation: optimization through response surface methodology, Mater. Today Proc. 72 (2023) 2697–2704, https://doi.org/10.1016/j.matpr.2022.09.031.
[89] G.K. Akkaya, Treatment of petroleum wastewater by electrocoagulation using scrap perforated (Fe-anode) and plate (Al and Fe-cathode) metals: optimization of operating parameters by RSM, Chem. Eng. Res. Des. 187 (2022) 261–275, https://doi.org/10.1016/j.cherd.2022.08.048.
[90] Y. Esfandyari, K. Saeb, A. Tavana, A. Rahnavard, F.G. Fahimi, Effective removal of cefazolin from hospital wastewater by electrocoagulation process, Water Sci. Technol. 80 (12) (2019) 2422–2429, https://doi.org/10.2166/wst.2020.003.
[91] U. Tezcan Un, A. Gul, S.E. Ocal, Optimization of electrocoagulation parameters for pretreatment of industrial metal cutting wastewater, Can. Int. J. Sci. Technol. (2017). ISSN 2356-9085.